3. SEISMOLOGICAL ASPECTS

Regional seismicity and historical earthquakes

New Zealand straddles the boundary of the Australian and Pacific plates, where relative plate motion is obliquely convergent across the plate boundary at about 50 mm/yr in the north of the country, 40 mm/yr in the center, and 30 mm/yr in the south (DeMets et al. 1994). The complex faulting associated with the changing orientation of the subduction zones in the northeast and southwest, causes predominantly dextral faulting through the axial tectonic belt in the center of the country.

As a result of this complex faulting, New Zealand is a region of distributed seismicity, in that the relative movement of the Australian and Pacific plates are not accommodated by one or two faults in a narrow zone, but by many faults across a much wider zone (the axial tectonic belt). It is therefore not surprising that both large historical earthquakes (Figure 3.1a), and recent seismicity (Figure 3.1b) occurred in almost any region in New Zealand.

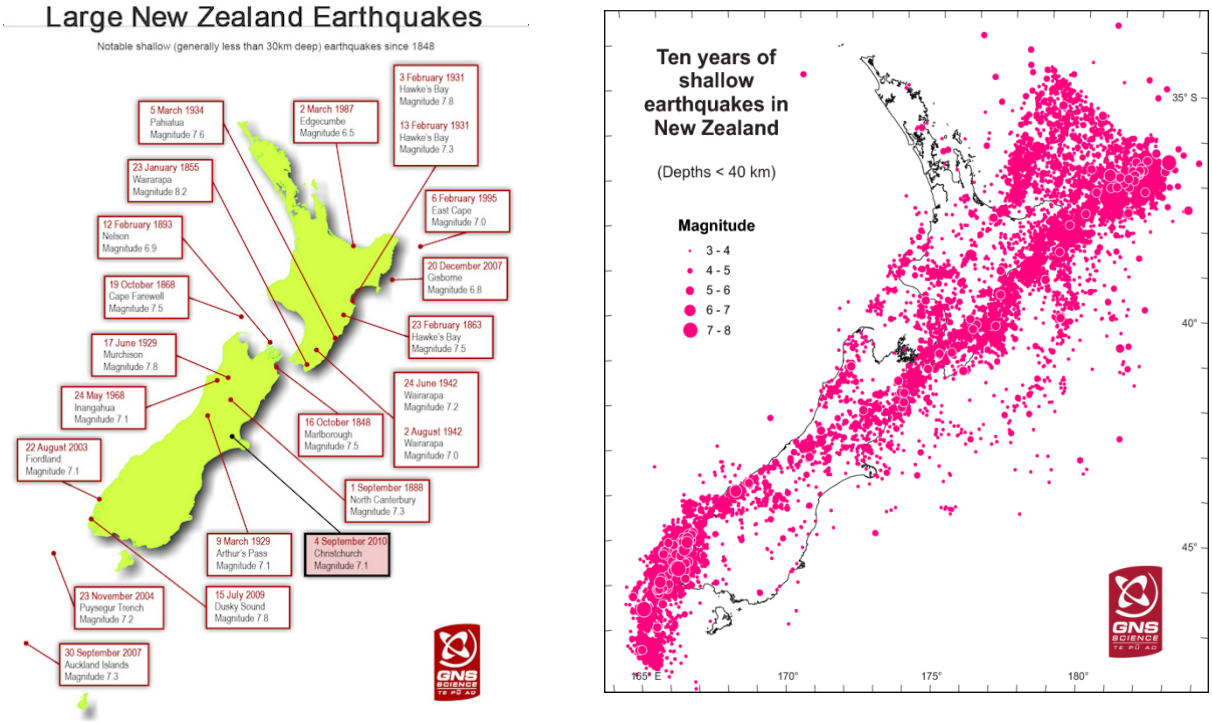

Figure 3.1 (a) Historical large earthquakes in New Zealand (http://sylph.gns.cri.nz/what/earthact/earthquakes/historic.html); and (b) shallow seismicity in the last ten years. (http://www.geonet.org.nz/earthquake/).

The 4 September 2010 M_w 7.1 Darfield Earthquake

The M_w7.1 Darfield earthquake occurred at 4:35am local time on the 4 September 2010. The epicenter was located at -43.55˚, 172.18˚, approximately 40 km to the west of Christchurch's the Central Business District (CBD) and about 80-90 km to the south and east of the current expression of the Australia - Pacific plate boundary through the island (the Alpine and Hope Faults). The faulting, on the newly-named Greendale Fault, was initially thought to be primarily dextral strike slip movement (as noted by both United States Geological Survey, USGS, and Earthquake Research Institute, ERI), with also some oblique reverse faulting (http://earthquake.usgs.gov/earthquakes/recenteqsww/Quakes/us2010atbj.php#summary).
However, GNS Science now believes the faulting to be of primarily a reverse mechanism (http://www.geonet.org.nz/news/article-sep-4-2010-christchurch-earthquake.html). Because the Canterbury plains are covered with river gravels, the surface expression of the Greendale Fault was not apparent, and therefore, its existence was unknown to earthquake geologists prior to the event.

Finite fault models

Finite fault models for the Darfield earthquake have been developed by several different organizations. Two publicly available inversions from USGS and ERI are shown in Figure 3.2 and Figure 3.3. Given that finite fault inversions are ill-conditioned, as expected, there are some differences between the models. However, both models illustrate that the nucleation point was approximately at the center of the ruptured fault plane. The resulting bi-lateral rupture therefore would have resulted in notably shorter duration of intense ground shaking at various locations, than would have occurred if the fault had have ruptured in a uni-lateral fashion. Both finite fault models also indicate one large asperity of high slip to the west of the epicenter. This is likely to have resulted in forward directivity effects observed in ground motions to the west of the fault, and backward directivity effects to the east of the fault (i.e. Christchurch).

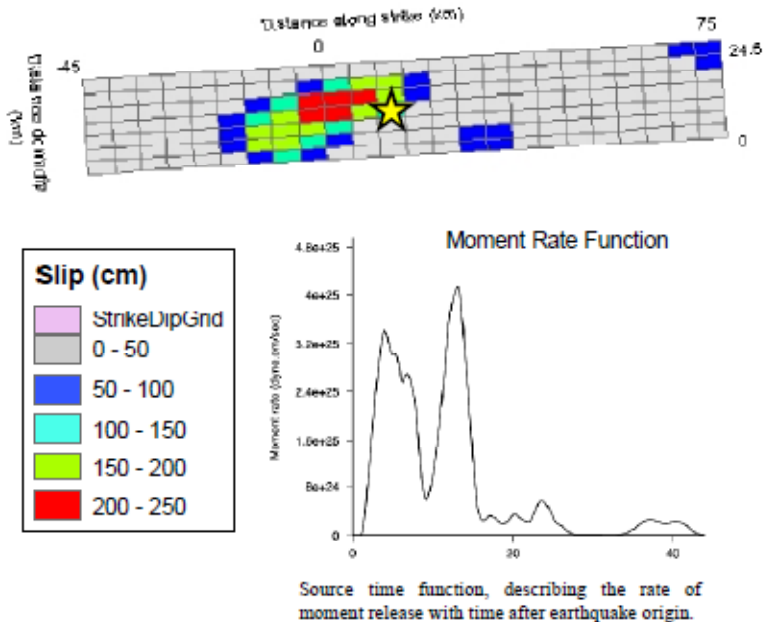

Figure 3.2 Finite fault inversion from Gavin Haynes (USGS).
(http://earthquake.usgs.gov/earthquakes/eqinthenews/2010/us2010atbj/finite_fault.php)

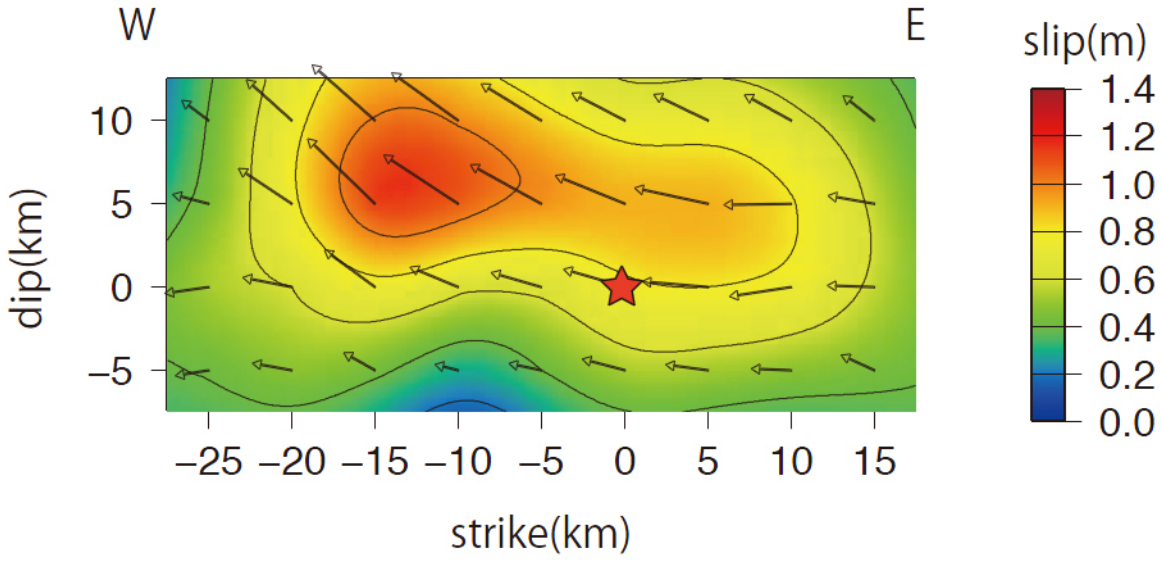

Figure 3.3 Finite fault inversion from ERI.

(http://outreach.eri.u-tokyo.ac.jp/2010/09/201009_nz_eng/)

Rupture dimensions and aftershocks

Geologists initially mapped the surface trace of the Greendale Fault as 22 km, but further work has found that now there is 29-km surface expression. As indicated by the finite fault models discussed in the previous chapter, the length of the fault rupture at depth is likely to be on the order of 40 km.

There have been numerous aftershocks recorded since the M_w7.1 mainshock. Figure 3.4 illustrates that the temporal occurrence of aftershocks has been in line with statistical predictions.

Figure 3.5 illustrates the distribution of earthquakes observed in the Canterbury region over the period 24 July – 24 September, which are primarily the result of the M_w7.1 mainshock and its aftershocks. It can be seen that the M_w7.1 mainshock has triggered many aftershocks on the edges of the Greendale fault, but also on many smaller faults in the general region. Although there is some speculation, it is generally considered that the occurrence of the M_w7.1 mainshock will result in little stress transfer effects to the primary faults in the axial tectonic belt (such as the Alpine fault).

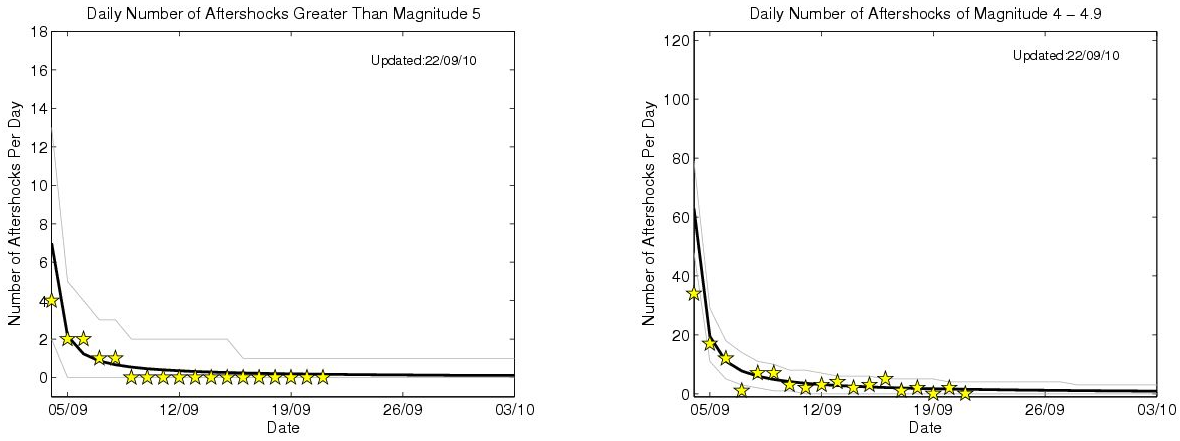

(a) (b)

Figure 3.4 Number of aftershocks with: (a) magnitude greater than 5; and (b) magnitude between 4 and 5, in comparison with statistical aftershock models (http://www.geonet.org.nz/news/sep-2010-darfield-earthquake/gns-science-response.html).

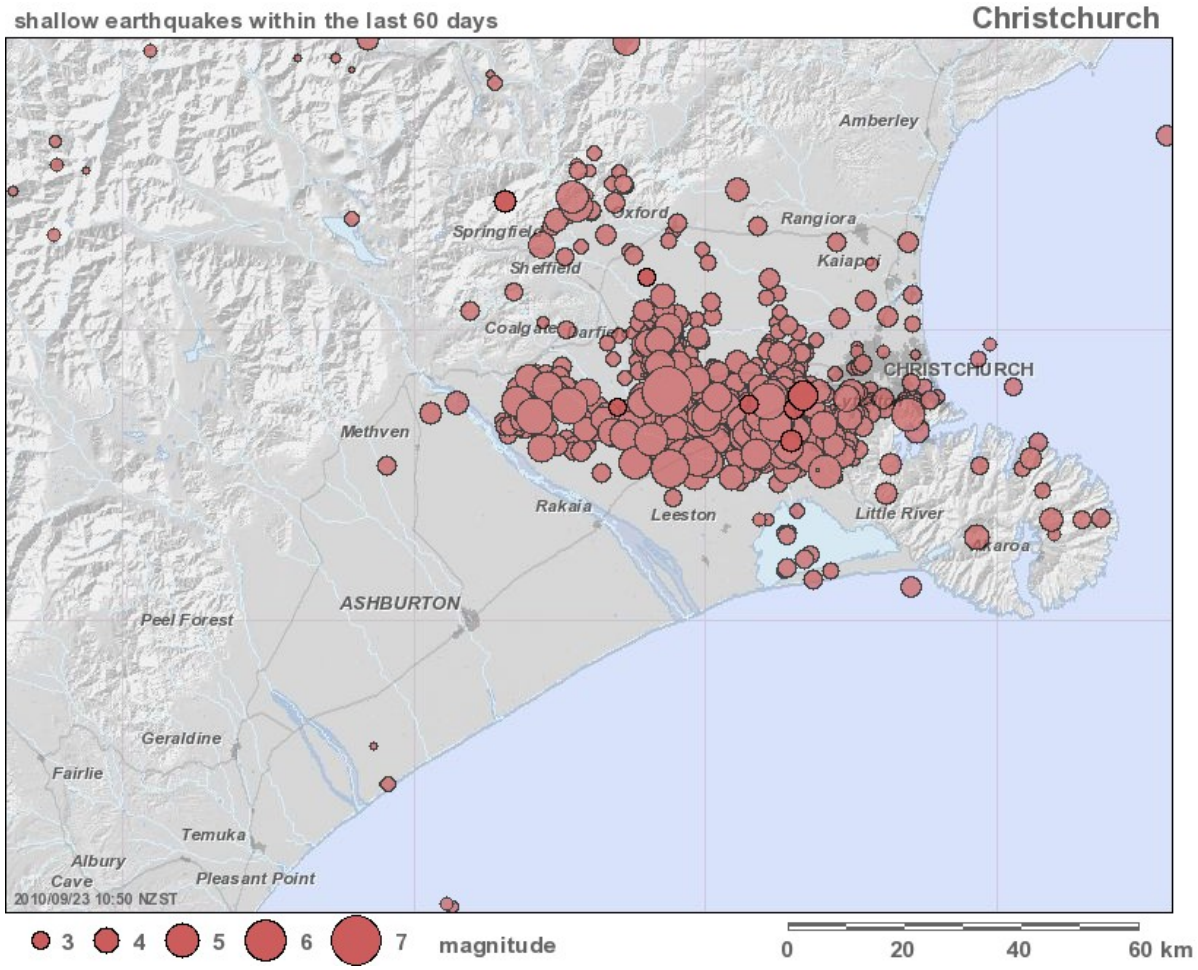

Figure 3.5 Location of earthquakes in the Canterbury region over the period 25 July – 24 September 2010 (i.e. primarily the mainshock and its aftershocks). (http://images.geonet.org.nz/maps/quakes/262-christchurch-quake.jpg)

Ground motion shaking

The ground motion shaking as a result of the mainshock was widely felt in the Canterbury region, and in New Zealand in general. Figure 3.6 illustrates the distribution of "felt-it" reports that were submitted online by the public. Figure 3.7 illustrates the USGS ShakeMap, which utilizes both predictive models of MMI, and also the publicly submitted "felt-it" report. It can be seen that MMI VIII-IX was observed in Darfield and Rolleston townships, and that the wider Christchurch region generally experienced MMI VI-VII.

Numerous people and authorities have contrasted the Darfield earthquake with the Haiti earthquake as an illustration of how adequate building standards and preparedness can lead to a

large difference in damage and casualties. However, comparison of MMI's observed to population exposures in Canterbury and Haiti dictates that caution should be made in such an interpretation (http://dotearth.blogs.nytimes.com/2010/09/07/in-earthquakes-poverty-population-and-motion-matter/).

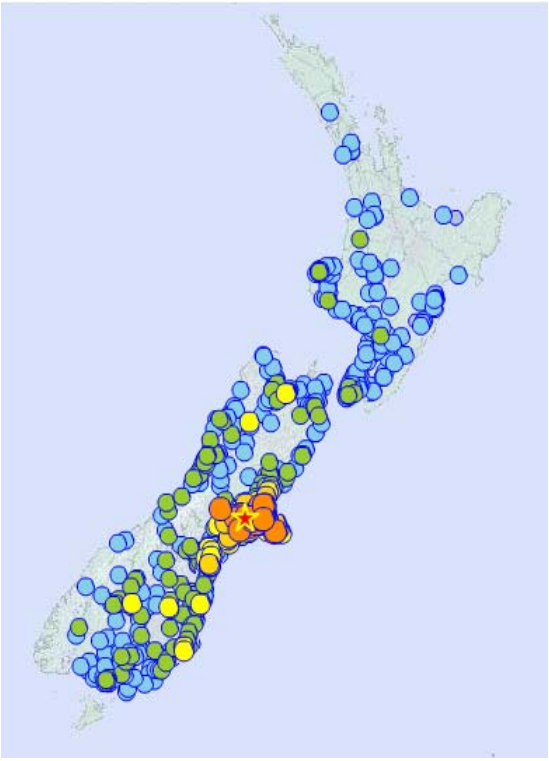

Figure 3.6 Locations of "felt-it" reports submitted online, there were 6897 reports as of 24 September 2010. (http://www.geonet.org.nz/earthquake/quakes/3366146g-shaking.html)

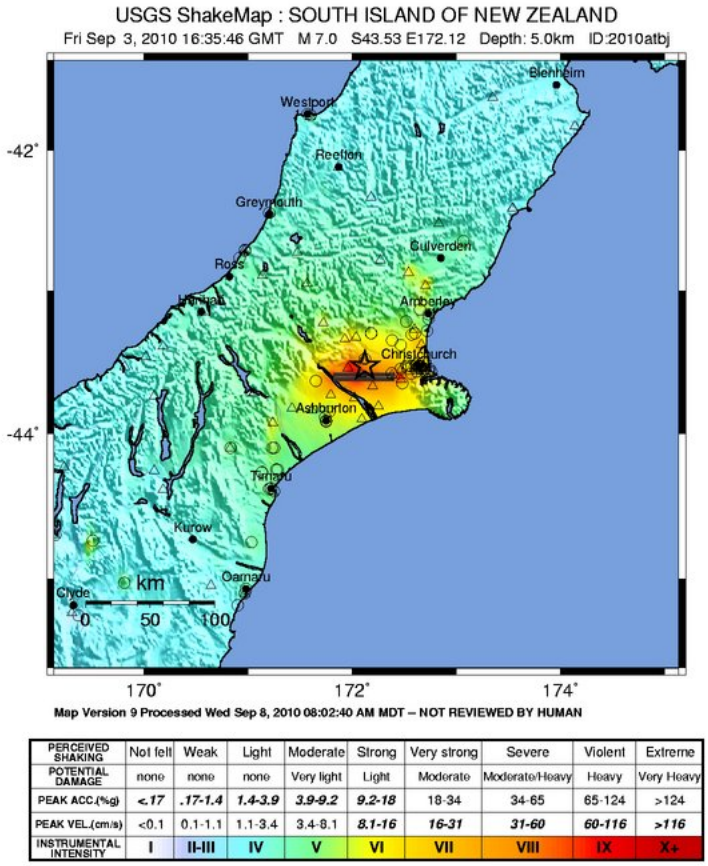

PERCEIVED SHAKING	Not felt	Weak	Light	Moderate	Strong	Very strong	Severe	Violent	Extreme
POTENTIAL DAMAGE	none	none	none	Very light	Light	Moderate	Moderate/Heavy	Heavy	Very Heavy
PEAK ACC.(%g)	*<.17*	*.17-1.4*	*1.4-3.9*	*3.9-9.2*	*9.2-18*	18-34	34-65	65-124	>124
PEAK VEL.(cm/s)	<0.1	0.1-1.1	1.1-3.4	3.4-8.1	*8.1-16*	*16-31*	*31-60*	*60-116*	*>116*
INSTRUMENTAL INTENSITY	I	II-III	IV	V	VI	VII	VIII	IX	X+

Figure 3.7 USGS ShakeMap from the M_w7.1 mainshock.
(http://earthquake.usgs.gov/earthquakes/shakemap/global/shake/2010atbj/).

The Canterbury region is well instrumented with strong motion seismographs. Figure 3.8 shows the vector-maximum peak ground accelerations (PGA_{VM}: Figure 3.8a) and the geometric mean of the peak horizontal ground accelerations ($PHGA_{GM}$: Figure 3.8b) that were recorded throughout the region. In the near source region, it can be seen that there are five PGA_{VM} recordings above 0.7g (although many of these peaks are in the vertical component). The maximum PGA_{VM} 1.25g recorded at the Greendale station has also been deemed to have been contaminated by falling debris in the house garage in which the seismograph is installed (J. Zhao, personal communication).

Using a wavelet decomposition procedure (Chanerley and Alexander, 2010) and integrating the Greendale record with and without the anomalous vertical peak at 35 seconds, Andrew Chanerley (pers comm.) finds that the horizontal velocities and displacements (x-displ. = -163.1 cm; y-displ. = -45.86 cm) are little affected, with the vertical integrated displacement ranging from -60.47 cm to -66.46 cm. This result suggests that falling debris-induced acceleration spikes

will have little effect on structural response computations (themselves integration processes). Further, the integrated permanent "fling" displacements are consistent with the field observations of 3-4 m offset (2 × 1.63 m = 3.26 m).

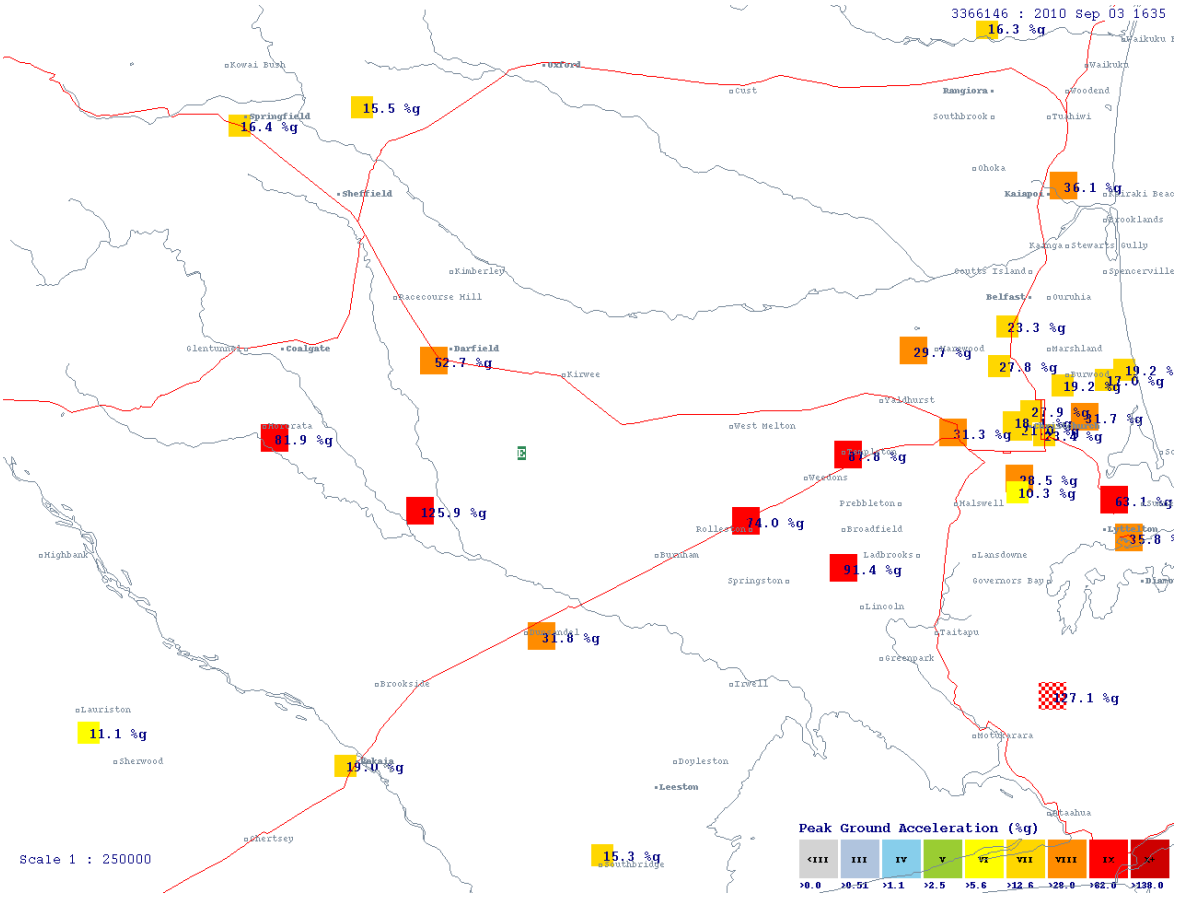

(a)

(b)

Figure 3.8 Peak ground accelerations recorded in the Canterbury region by strong motion seismographs: (a) Vector-maximum peak ground accelerations (PGA_{VM}) and (b) Geometric mean of peak horizontal ground accelerations ($PHGA_{GM}$). The surface rupture of the fault and the epicenter are superimposed on the image. From the left to right edge of the image is ~123 km. (http://www.geonet.org.nz/news/sep-2010-darfield-earthquake/gns-science-response.html).

Figure 3.9 illustrates a preliminary comparison between the attenuation of ground motion intensity with source-to-site distance. The comparison is preliminary in that, as previously mentioned, many details of the fault rupture (i.e. the fault plane and faulting mechanism) have not been finalized. Acceleration Spectrum Intensity (ASI), defined as the integral of the pseudospectral acceleration of a ground motion from 0.1 to 0.5 sec (Von Thun et al. 1988), shown in Figure 3.9a illustrates somewhat of a high-frequency average of a ground motion, while Spectrum Intensity (SI), defined as the integral of pseudospectral velocity of a ground motion from 0.1 to 2.5 sec (Housner 1952), shown in Figure 3.9b illustrates a moderate frequency average of a ground motion. It can be seen that the ground motions from this event by

and large conform to predictions from empirical ground motion prediction equations. There is however clearly variability in the motion amplitudes that occur as a result of near-source effects, topography and basin effects, and near-surface nonlinearities in the soft glacial deposited soils that underlie the Christchurch region.

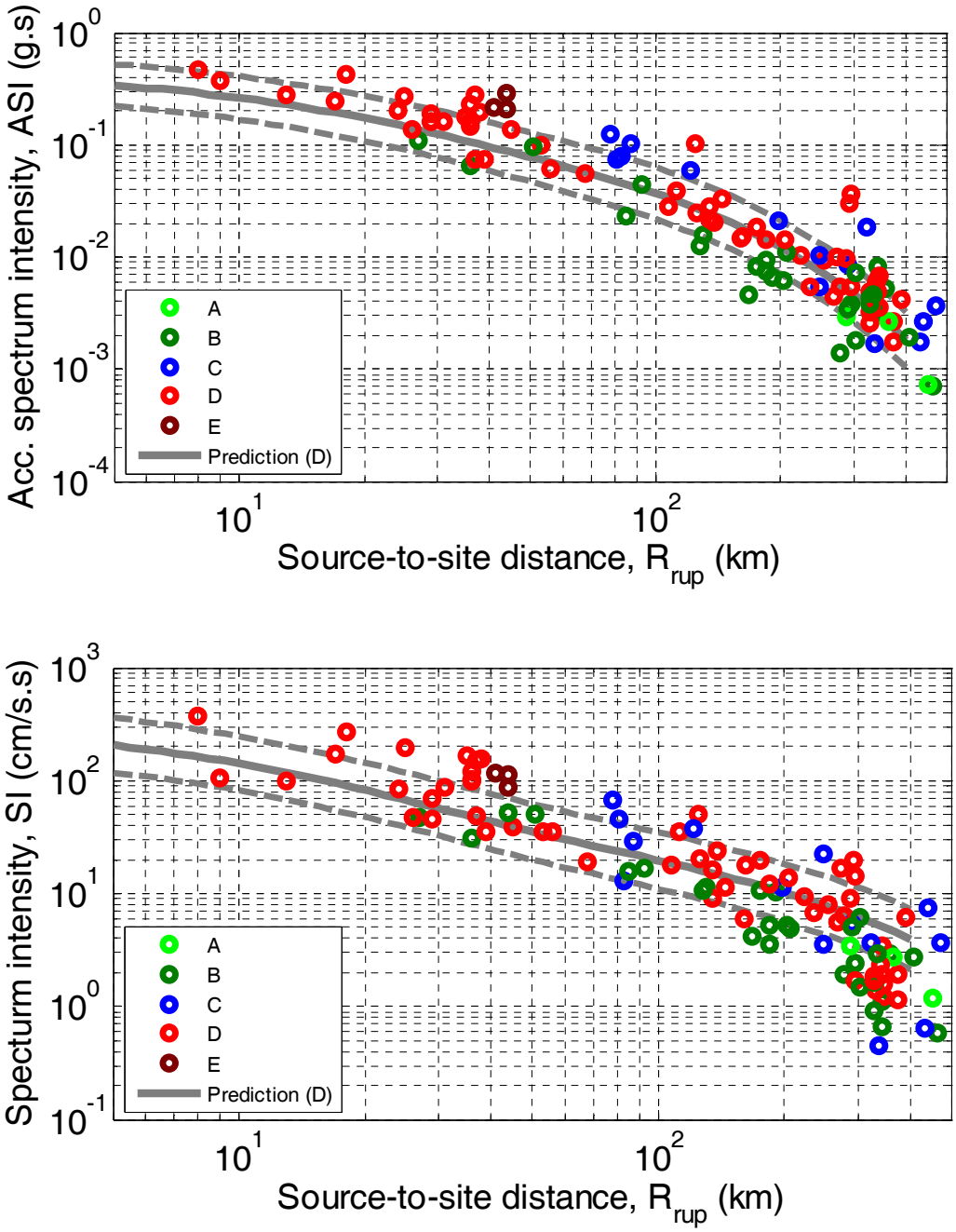

Figure 3.9 Observations of ground motion intensity compared with empirical prediction equations. The predictive relation for ASI and SI are a NZ-specific modification of the Chiou and Youngs (2008) model.

Figure 3.10, Figure 3.11, and Figure 3.12 illustrate the recorded acceleration time histories and respective response spectra at the Greendale, Christchurch hospital, and Kaiapoi strong-motion stations. Also shown for reference are the predicted response spectra from ground motion prediction equations (Brendon Bradley, pers. comm.). Locations of these seismographs can be found at: http://www.geonet.org.nz/resources/network/netmap.html.

The Greendale seismograph was located almost directly over the fault plane and recorded the strongest ground motion from the mainshock. It can be seen from the horizontal components of the ground motion that cyclic mobility in surficial soil layers may have occurred during the strong ground shaking. The occurrence of cyclic mobility is indicated by the high frequency spikes in the later half of the strong motion record. The spectral accelerations for this set of ground motion records are in line with empirical predictions.

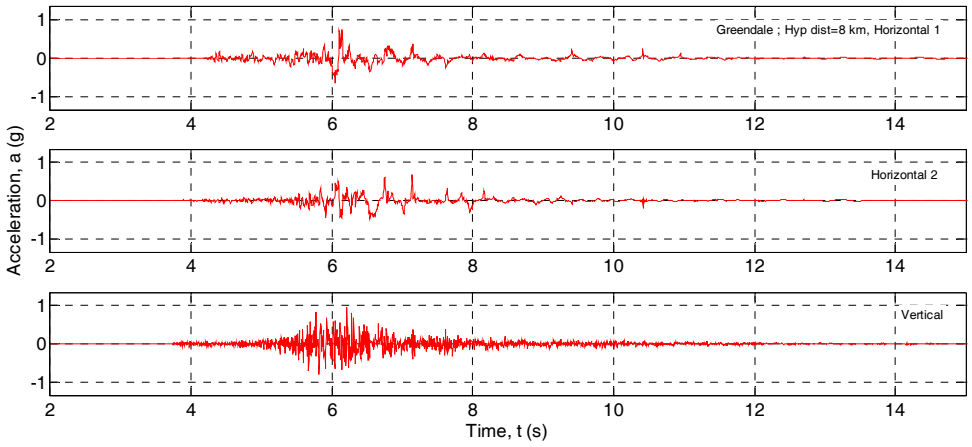

(a)

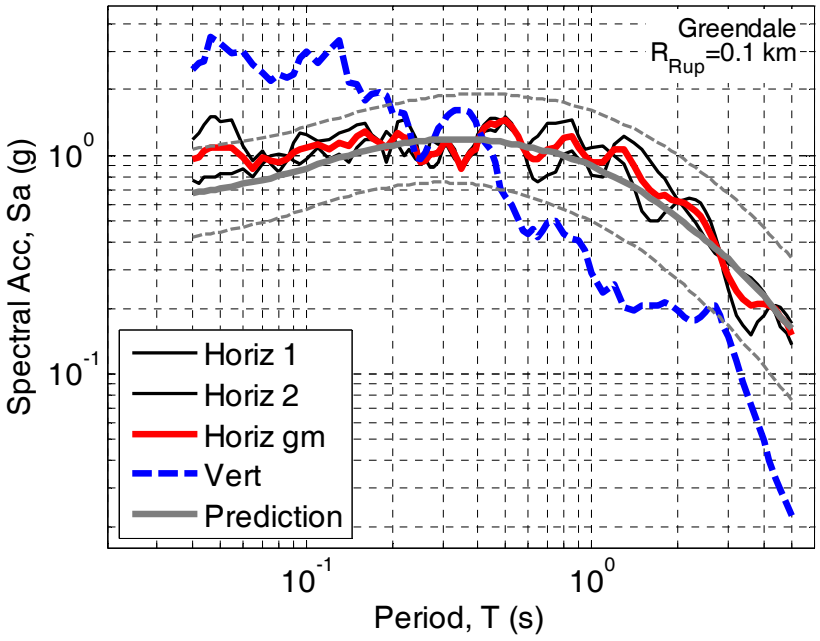

(b)

Figure 3.10 Motions recorded by the Greendale seismograph: (a) Acceleration time-histories; and (b) response spectra (Note that "Horiz gm" is the geometric mean of the two horiziontal components of motion.).

The Christchurch hospital seismograph is located near the center of Christchurch. The response spectra from this station clearly illustrate the significance of basin effects on the spectral amplitudes at 2-3 second vibration periods. Additionally, the spectral peak at 0.3-0.5 seconds is likely due to the near-surface sediments, which were rapidly deposited in the post-glacial period.

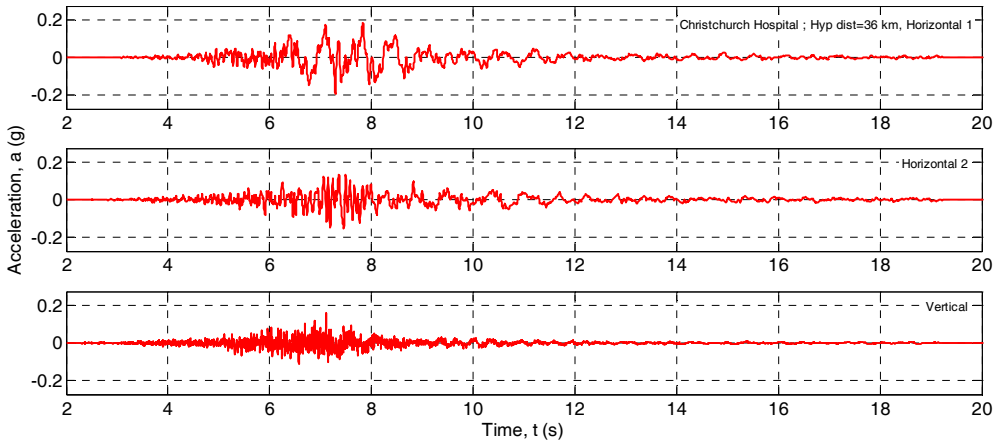

(a)

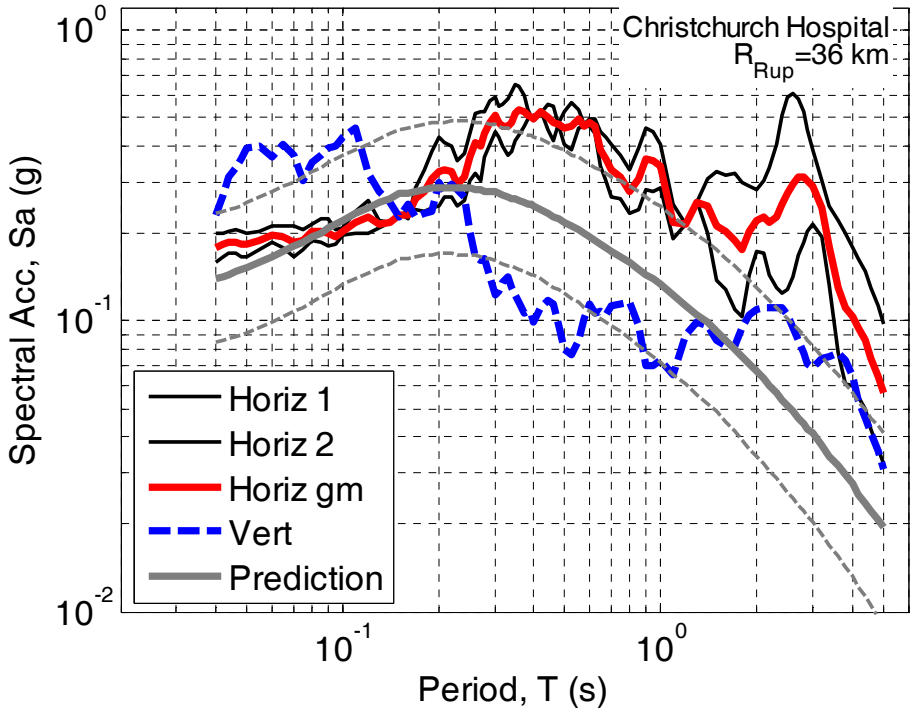

(b)

Figure 3.11 Motions recorded by the Christchurch hospital seismograph: (a) Acceleration time-histories; and (b) response spectra. (Note that "Horiz gm" is the geometric mean of the two horiziontal components of motion.).

The Kaiapoi seismometer is located in the town of Kaiapoi, which experienced substantial liquefaction and lateral spreading. It can be seen that the ground motions observed are generally

well above those predicted by empirical models, indicating the importance of near surface sediments on site amplification.

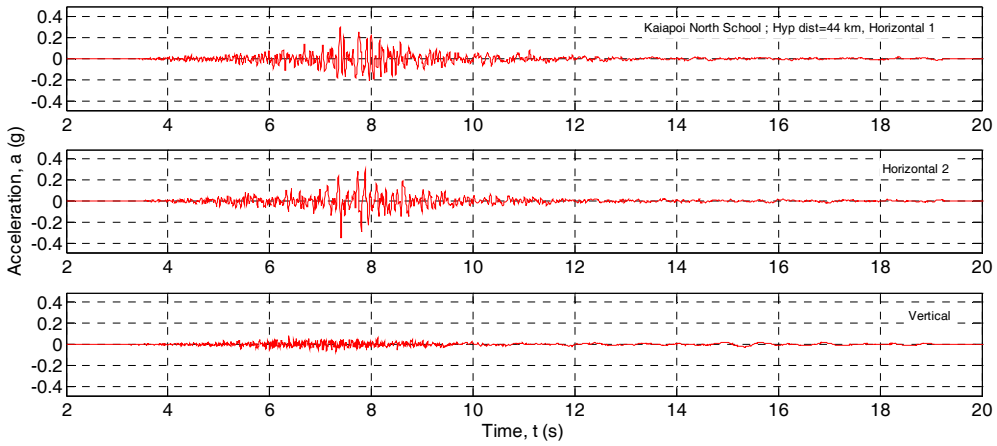

(a)

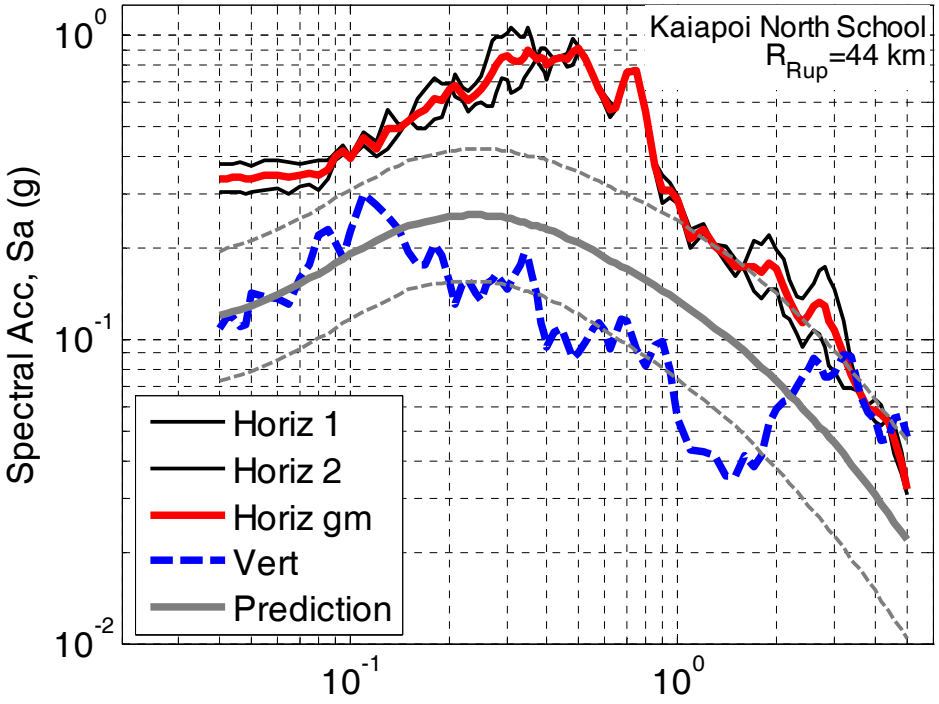

(b)

Figure 3.12 Motions recorded by the Kaiapoi seismograph: (a) Acceleration time-histories; and (b) response spectra. (Note that "Horiz gm" is the geometric mean of the two horizontal components of motion.).

References

Chanerley, A.A. and Alexander, N.A. (2010). Obtaining estimates of the low-frequency ‘fling’, instrument tilts and displacement timeseries using wavelet decomposition, *Bull Earthquake Eng*, 8, 231–255.

Chiou, B.S.J. and Youngs, R.R. (2008). An NGA Model for the average horizontal component of peak ground motion and response spectra, *Earthquake Spectra*, 24, 173-215.

DeMets, C., Gordon, R.G., Argus, D.F., Stein, S. (1994). Effect of recent revisions to the geomagnetic time scale on estimates of current plate motion, *Geophysical Research Letters*, 21, 2191-2194.

Housner, G.W. (1952). Spectrum Intensities of Strong-Motion Earthquakes, *Proc. Symp. Eathquake and Blast Effects on Structures*, Engineering Research Institute, Los Angeles.

Von Thun, J., Roehm, L., Scott, G., and Wilson, J. (1988). Earthquake Ground Motions for Design and Analysis of Dams, *Earthquake Engineering and Soil Dynamics II - Recent Advances in Ground Motion Evaluation*, Geotechnical Special Publication 20, 463-481.